OVERVIEW OF THE OUTER RADIATION BELT DOSE RATES, OBSERVED AT SPACE STATION "MIR" AND AT THE INTERNATIONAL SPACE STATION BY LIULIN TYPE INSTRUMENTS

Tsvetan Dachev[1], Borislav Tomov[1], Yuriy Matviichuk[1], Plamen Dimitrov[1], Yordanka Semkova[1], Malina Yordanova[1], Nikolay Bankov[1], Mityo Mitev[1], Vyacheslav Shurshakov[2], Viktor Bengin[2]

[1]Space Research and Technology Institute – Bulgarian Academy of Sciences
[2]Institute for Biomedical Problems – Russian Academy of Sciences
e-mail: tdachev59@gmail.com

Keywords: *Earth's radiation belts, International Space Station, Space radiation dose*

Abstract: *Cosmic radiation doses from relativistic electrons from the outer radiation belt (ORB) outside the International Space Station (ISS) and the Photon M2/M3 satellites were first reported [1] by a team from SRTI-BAS in 2009. This paper aims to analyze the dose rates from the ORB of the manned stations "MIR" and the ISS, to confirm their constant presence and to emphasize the significance of these studies.*

Special attention is paid to the dose variations in two features in the ORB: precipitation bands of relativistic electrons and relativistic electrons penetration from the ORB at low L-values and in the inner radiation belt.

АНАЛИЗ НА МОЩНОСТИТЕ НА ДОЗИТЕ ОТ ВЪНШНИЯ РАДИАЦИОНЕН ПОЯС, НАБЛЮДАВАНИ НА СТАНЦИЯ „МИР" И НА МЕЖДУНАРОДНАТА КОСМИЧЕСКА СТАНЦИЯ С ПРИБОРИ ОТ ТИПА ЛЮЛИН

Цветан Дачев[1], Борислав Томов[1], Юрий Матвийчук[1], Пламен Димитров[1], Йорданка Семкова[1], Малина Йорданова[1], Николай Банков[1], Митьо Митев[1], Вячеслав Шуршаков[2], Виктор Бенгин[2]

[1]Институт за космически изследвания и технологии – Българска академия на науките
[2]Институт за медико-биологически проблеми – Руска академия на науките
e-mail: tdachev59@gmail.com

Ключови думи: *Радиационни пояси на Земята, Международна космическа станция, доза космическа радиация*

Резюме: *Дозите космическа радиация от енергетичните електрони от външния радиационен пояс (ВнРП) извън Международната космическа станция (МКС) и спътниците Фотон М2/М3 са докладвани за първи път в статия [1] на колектив от ИКИТ-БАН през 2009 г. Настоящата статия цели да анализира мощностите на дозите от ВнРП на пилотируемите станции „МИР" и МКС; да потвърди тяхното постоянно наличие и подчертае значимостта на този тип изследвания.*

Специално внимание се обръща на вариациите на дозата в две характеристики в ВнРП: лентите от релативистични електрони и на проникването на релативистични електрони от ВнРП в ниски L-стойности и във вътрешния радиационен пояс.

Introduction

The dominant radiation component in near the Earth space environment are the galactic cosmic rays (GCR), modulated by the solar activity. The GCR are charged particles that originate from sources beyond our solar system. These particles are accelerated by high energetic sources like neutron star, black holes and supernovae within our Galaxy. GCR are the most penetrating of all

major types of ionizing radiation. The energies of GCR particles range from several tens up to 10^{12} MeV nucleon^{-1}.

Radiation belts are the regions of high concentration of energetic electrons and protons trapped within the Earth's magnetosphere. The inner radiation belt (IRB), located between about 0.1 to 2 Earth radii, consists of both electrons with energies up to 10 MeV and protons with energies up to ~400 MeV. The protons from the inner radiation belt contribute to the main absorbed dose inside the ISS. The outer radiation belt (ORB) starts from about 4 Earth radii and extends to about 9-10 Earth radii in the anti-sun direction. It consists mainly of high-energy (0.1–10 MeV) electrons. The electron flux may cause problems for components located outside a spacecraft (e.g. solar cell degradation). These electrons do not have enough energy to penetrate the heavily shielded spacecraft as is the case with the ISS wall, but they may give large additional doses to astronauts during extra vehicular activity (EVA) [1-4].

The solar energetic particles (SEP) are mainly produced by solar flares, sudden sporadic eruptions of the chromosphere of the Sun. High fluxes of charged particles (mostly protons, some electrons and helium and heavier ions) with energies up to several GeV are emitted by processes of acceleration outside the Sun. The time profile of a typical SEP starts with a rapid exponential increase in flux, reaching a peak in minutes to hours. The energy emitted are up to few hundred MeV nucleon^{-1} and the intensity can reach 10^4 cm^{-2} s^{-1} sr^{-1}.

Instruments description

The data from four different Liulin type instruments were used in this study.

LIULIN instrument [2] (pls. look Fig. 1, panel 1.1) was designed in 1986-1988 and used on "MIR" space station from April 1988 till August 1994. Its measurements were based on a single silicon detector followed by a charge-sensitive shaping amplifier (CSA) AMPTEK A225 type (https://www.amptek.com/internal-products/a225-charge-sensitive-preamplifier-shaping-amplifier). The number of the pulses at the output of the CSA above a given threshold was proportional to the particle flux hitting the detector. The amplitude of the pulses at the output of the CSA was proportional to the particles' deposited energy. The integral of the energy depositions of the particles accumulated in the detector during the measurement interval allowed the calculation of the dose rate.

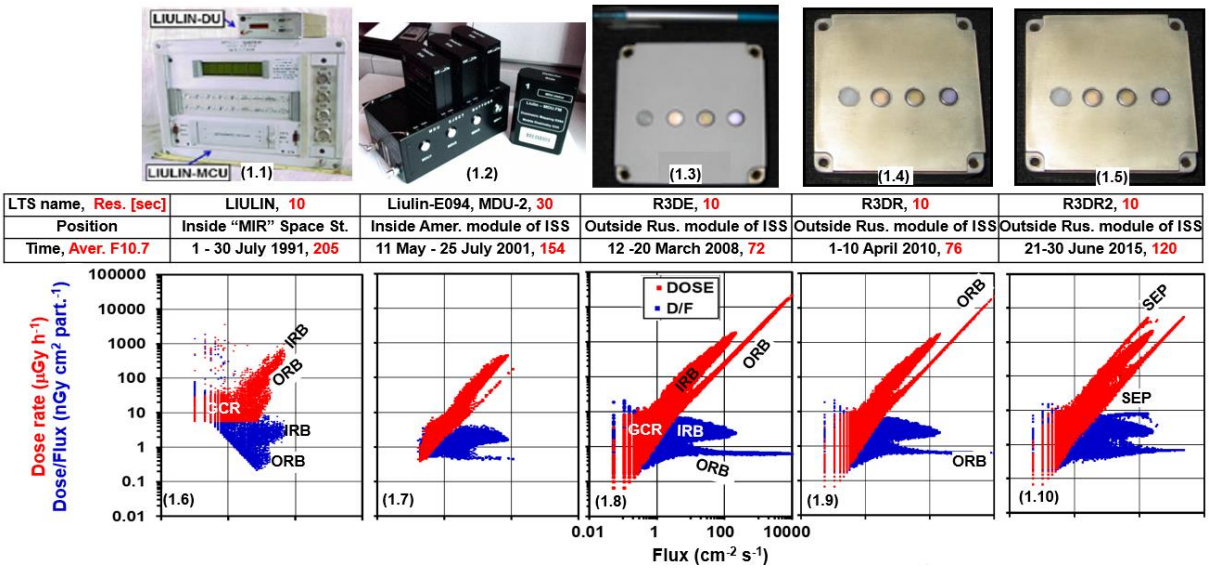

Fig. 1. Comparison of data obtained by five experiments on "MIR" and ISS in the period July 1991-June 2015

The Mobile Radiation Exposure Control System Liulin-E094 [3] (Fig. 1, panel 1.2) was a part of the experiment Dosimetric Mapping E094. The latter was placed in the US Laboratory module as a part of the Human Research Facility of Expedition Two Mission 5A.1, STS-102 Space Shuttle Flight. The system consists of four Mobile Dosimetry Units (MDU) and one Control and Interface Unit (CIU). Data from MDU number 2 (MDU-2) are used in this study. The MDU contains: one semiconductor detector with 0.3 mm thickness and 2.0 cm^2 area Canberra RF-14*14- 300-EB type; one low noise, hybrid, charge-sensitive preamplifier A225 type of AMPTEK Inc.; a fast 12 channel ADC; 2 microcontrollers and an 0.5 MB flash memory. The unit is managed by through specially developed software. The pulse amplitudes are proportional by a factor of 240 mV/MeV according to the AMPTEK A225F preamplifier specifications (A225 Specs for pdf (fastcomtec.com). The amplitudes are digitized

and organized in a 256-channel spectrum. Using the System International (SI) definition, the dose D (in Grey) is calculated from the sum of 256 channels amplitudes in MeV divided by the mass of the detector in kilograms.

The European Space Agency (ESA) EXPOSE-E, EXPOSE-R and EXPOSE-R2 facilities accommodated three Bulgarian-German Radiation Risk Radiometer-Dosimeters (R3D). R3DE instrument [4] (pls. look Fig. 1, panel 1.3) was used inside the EXPOSE-E facility on the Columbus module of the ISS in 2008-2009. R3DR spectrometer [5] (Fig. 1, panel 1.4) worked inside the EXPOSE-R facility from 2009 to 2010. R3DR2 is the same instrument as R3DR. It was part of EXPOSE-R2 facility on the ISS from 2014 until 2016 [6]. The extension "R2", same as for the EXPOSE-R2 facilities, is used to distinguish its data from the data from the previous mission. The two R3D spectrometers were built, applying the same schematics as that described in the previous paragraph for Liulin-E094, MDU-2 instrument. The detectors in the R3D spectrometers are Hamamatsu S2744-08 silicon PIN photodiodes (Si PIN photodiode S2744-08 | Hamamatsu Photonics).

Identification of energetic electrons from ORB during analyzed experiments on "MIR" and ISS

Fig. 1 compares data from "MIR" and ISS from the period 1991 – 2015. It has five columns and three rows. Each column presents the data got by the Liulin type spectrometers (LTS), illustrated on the first row. The second row includes a table giving information for: LTS name, the resolution in seconds, the position on the station, the time resolution of the measurements in seconds and the averaged in the observed time interval solar radio flux (F10.7) in solar flux units (Solar Cycle Progression | NOAA / NWS Space Weather Prediction Center). The third row contains graphics of the variations of the Dose rate and Dose to Flux ratio in dependence by the Flux.

Historically during the analysis of the LTS data, it was found that the graphics of the variations of the Dose rate and Dose to Flux ratio in dependence by the Flux have a similar feature as those depicted in panels (1.6)-(1.10) of Fig. 1. These five similar graphics are our major proof that we have observed fluxes of energetic electrons from the ORB in all experiments.

The explanation of the graphics in the Panels (1.6)-(1.10) is as follows: On the horizontal axis is the flux in cm^{-2} s^{-1}, while on the vertical axes are two parameters: the dose rate in μGy h^{-1} (in red points) and the dose to flux ratio in nGy cm^2 $particle^{-1}$ (in blue points). These type of graphics allows visualizing the four different radiation sources components expected in the stations altitudes in the range 390-450 km. They are GCR particles, protons with more than 15.8 MeV energy in the (South Atlantic Anomaly) SAA region of the IRB, relativistic electrons with energies above 0.78 MeV in the ORB and solar energetic particles (SEP) [6].

The large number of experimental points in the diagonal of the figures is responsible for the dose rate values, which, as expected, are linearly dependent on the flux, while the number of points lying almost horizontally represent the dose to flux ratio (D/F) ratio. Both graphics are with a form of large area in the small values and two maxima in the high values. The large number of the measured points are in the range 0.03–30-μGy h^{-1} and for a fixed flux, a wide range of doses is observed. These two features could be explained only by GCR particles, which, being relatively less abundant and having high linear energy transfer (LET), deposit, varying doses for the same flux. The smallest dose rates (0.03–0.430-μGy h^{-1}) are observed close to the magnetic equator, while the largest ones are observed at high latitudes. In the horizontal graphic, this part of the data is represented with a similarly large number of points, which in bigger part overlaps the dose rate diagonal points.

The lower maxima is in the dose rate range 9–22,000-μGy h^{-1} and takes the form of a straight line. Its representation in the horizontal graphic is a maxima extending up to 10,000 cm^{-2} s^{-1}, with dose to flux values below 1 nGy cm^2 $particle^{-1}$. This maximum is based on low LET particles and could be formed only by relativistic electrons [1] in the outer radiation belt.

The upper maximum in the diagonal graphic has a different source than the previous two. A high range of doses for a fixed flux characterizes it but the dose rates are in the range 30–1900-μGy h^{-1}. This number of points could only represent protons from the IRB (in the region of the SAA) whose dose depositions depend on the energy. The lower energy protons deposit higher doses. In the horizontal graphic, this maximum has a similar form and is situated in the range 1.2–8-nGy cm^2 $particle^{-1}$. In Panel (1.6) a third maximum appears in both graphics. This maximum is generated by SEP protons.

Straight lines can approximate both IRB and ORB maxima. From these approximations, we calculate that one proton in the IRB deposits, on average, a dose of 1.4 nGy in the silicon detector, while one electron in the ORB deposits a dose of 0,33 Gy. This is in good agreement with Heffner's formulae [6, 8].

The conclusion, which can be drawn from of the graphics in the Panels (1.6)-(1.10) is that the data can be simply split in two parts by the requirements for the ratio *D*/*F*<1 and *D*/*F*>1-nGy cm^2 particle^{-1} [6, 8]. This will generate results that will split the IRB and ORB sources. Looking on the graphics in the Panels (1.6)-(1.10) it is seen that the D/F maxima corresponding to the ORB energetic electrons are situated in region of lover than 1-nGy cm^2 particle^{-1}, while the IRB D/F maxima are seen in the region higher than 1-nGy cm^2 particle^{-1}.

GCR protons in equatorial and low latitude regions have very small fluxes of less than 1 nGy cm^2 particle^{-1}. That is why the D/F ratio is not stable and varies in the range from 0.03 to 30 nGy cm^2 particle^{-1}. This large variation makes the *D*/*F* ratio inapplicable for the characterization of the GCR radiation.

Peculiarities of ISS ORB

The result of the separation of the four radiation sources (including SEP) is seen in Fig. 2. It presents the latitudinal distribution of the dose rates against McIlwain's L values [7]. The L value is plotted on the x-axis. On the y-axis, the absorbed dose rate, measured by the R3DR2 instrument, is depicted. Fig. 2 demonstrates the data from 1st to 10th of June 2015. The picture contains 86,400 points at a 10 s resolution (10 days × (360 × 24 (h)). Four different primary radiation sources separated by the heavy black lines are seen. These sources are illustrated in Fig. 2 with different colours, i.e. IRB (green), ORB (blue), GCR (red) and SEP (magenta). From one 10 s independent measurement of the dose rate (D) and flux (F), we were able to calculate one dose to flux ratio (D/F). Using this, we were able to decide only what the predominant radiation sources were, but we were unable to extract the exact doses of each source. The black line in Fig. 2 are generated by the operator and the interactive separation software [6].

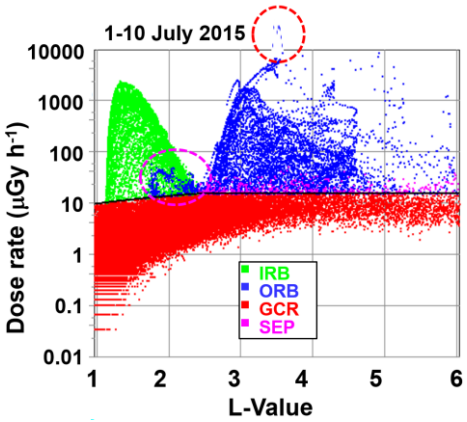

Fig. 2. The two peculiarities in the ORB: The dashed red oval line in the upper part of the figure marks the relativistic electron precipitations (REP), while the dashed magenta oval in the middle-left part of the figure displays the penetration of relativistic electrons in low L-values and in the IRB

The above data are from R3DR2 instrument on the ISS. R3DR2 studies two features of the ORB in the period 2014-2016. They are (1) the precipitation bands (PB), seen in the red oval at the top of Fig. 2, and (2) the penetration of relativistic electrons from the ORB to the low L-values and the IRB (PRE), marked in the magenta oval in the left central part of the figure.

The GCR source are the majority of the measurements in Fig. 2. The latter are seen as the area with many red points in the bottom part of the figure over the L value range between 1 and 6. The dose rates in the GCR region vary between 0.03 and 15-μGy h^{-1}. The second permanent source of radiation corresponds to the protons in the SAA region of the IRB, which are situated as a large maximum (green points) in the upper left corner of Fig. 2, with a total of 5,876 points. They cover L values between 1.2 and 2.6.

Fig. 2 presents the most dynamic 10 days of the ORB source distribution in L-values for the entire period of observations between November 2014 and January 2016. High dose rate patches are seen. The largest penetration of relativistic electrons below L=2 is observed in the dashed magenta oval. Also, in the dashed red line oval in the top part of the figure points with dose rate values larger than 10,000-μGy h^{-1} are seen. This according to our classification in [9] is indication of precipitation bands [10].

Long-term variations of the ORB peculiarities, registered at the ISS

Fig. 3 contains two 3D L and time graphics with different maximal flux ranges as seen by the two color code bars in the right and left side of the panels. The Panel (3.1) presents the variations of the maximal observed, in the bin, relativistic electron flux data (in cm^{-2} s^{-1}) against the colour bar in the left-upper part of the figure. The bins with size of 0.02 L value units are organized in a 442 daily vertical bars. They extend between L equal to one and six against the horizontal date axes. The ISS maximal flux bins cover the whole L values range from 1 to 6 in the Southern hemisphere, while in the Northern hemisphere the flux data bins are extended only up to L= 4.7, because of the Earth magnetic field hemisphere asymmetries. This explains the borderline seen in Panel (3.1) at L=4.7 and the smaller population of bins in the L range between 4.7 and 6.

The white line curve in the panel (3.1) presents the variations of the Dst-index in nanotesla (http://wdc.kugi.kyoto-uac.jp/index.html). Well-seen is the correlation between the Dst-index and the ORB maximal flux and the equatorialward boundary [6].

The magenta circles spread at different L-values show the position of the PB in the outer belt. The PB is identified as rapid (10–40-s) dose rate enhancement from the normal (20–200 μGy h^{-1}) outer radiation belt (ORB) level and similar fast return to the same low level. Only PBs that have in the time profile dose rates larger than 10,000-μGy h^{-1}, identical to flux larger than 4000 cm^{-2} s^{-1}, for 10 or more seconds were selected. Sixteen PBs were studied. The largest selected PB was registered by the R3DR2 instruments. R3DR2 detector was behind 0.3 g cm^{-2} shielding. The dose of the PB was 464 μGy for 70 s. The later is larger than the ORB daily average dose rates for 366 days, based on 442 days measurements during the analysed period. The daily average doses inside of the ISS were measured, using the DOSTEL instrument, at an average level of 194-μGy d^{-1} [11]. This indicates that only for 70 s, the cosmonaut/astronaut, being on extra vehicular activity (EVA), where they are shielded only by their space suits, will accumulate the equivalent of about 2.5-days dose inside of the ISS.

The green-blue points seen in panel (3.1) at L-values below 2.4 are the locations of the penetrations of relativistic electrons identified in the colour bar of panel (3.1).

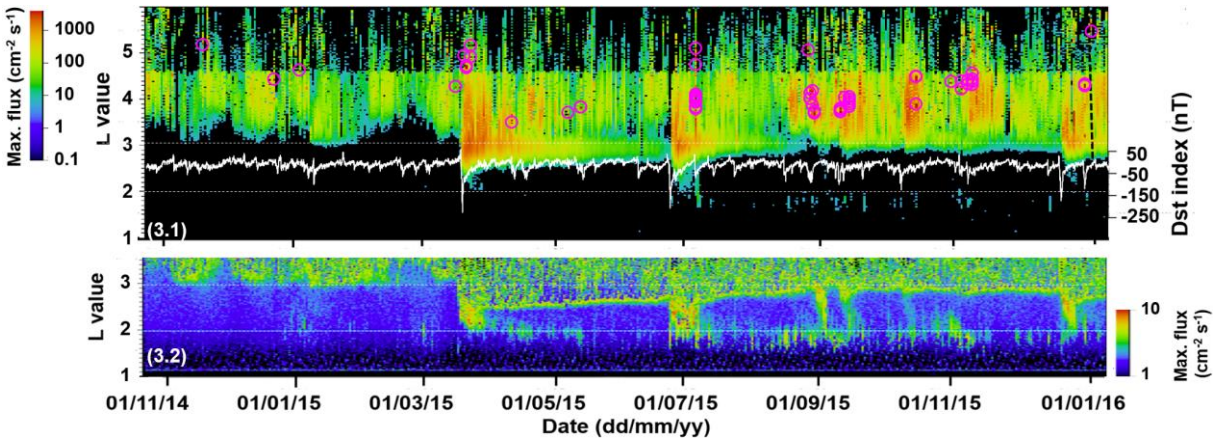

Fig. 3. The two panels are dedicated to the long-term variations in the ISS ORB features: Panel (3.1) illustrates the precipitation bands (seen with magenta circles); Panel (3.2) shows the penetration of relativistic electrons in the low L-values and the IRB.

The Panel (3.2) in the L range from 1.2 to 3.6 presents the whole dynamics of the penetrations of relativistic electrons between 24 October 2014 and 16 January 2016. The color bar on the right side of Fig. 3.2 allows much better identification.

Similarly to Claudepierre et al. [12], we recorded the first strong penetration of the relativistic electrons below L=2.5 on March 18, 2015. In the period March 18–28 2015 the lowest boundary of L=1.7 was reached. Then the relativistic electrons at low L disappeared on March 28, 2015. The storm on June 25, 2015 moved again the fluxes of the ORB relativistic electrons at L-values below two. They are well seen in the lower part of Panel (3.2). The ORB enhancement on July 4, 2015 emphasized them again but at this case the minimal L-values reached was L=1.6. Almost all disturbances in the Dst-index from July 11, 2015 until January 1, 2016 generated a new portion of relativistic electrons in the range of L-values between 1.6 and 2. They existed for few days and disappeared until the next Dst-index disturbance and magnetic substorm.

Conclusions

The main conclusion of the presented data is that the ORB enhancements, the PBs events and the penetrations of relativistic electrons at low L-values and in the IRB are common on the manned “MIR” and ISS space stations. Although the obtained doses do not pose extreme risks for the astronauts, being on EVA, they have to be considered as a permanently detected radiation source, which requires additional comprehensive investigations.

Acknowledgements

The authors thank to all Bulgarian and foreign specialists and organizations that participated in the development of the Liulin instruments; to our international partners for the financing of projects related to the creation of Liulin equipment; to the astronauts and cosmonauts aboard the manned space stations “Mir” and ISS for conducting experiments with Liulin equipment.

Data availability

The data, used in this paper, are part of the “Unified web-based database with Liulin-type instruments” that are available online, free of charge at the following URL: http://esa-pro.space.bas.bg/database.

The database contains data from nine Liulin type experiments around the Earth and Liulin-MO data in the path to Mars (2016–2017) and in Mars orbit (Since 2017) [13]. Each data point comprises up to 256 parameters, which except the measured values, listed the time and space parameters of the carrier, which characterize the data.

References:

1. Dachev, T. P., B. T. Tomov, Yu. N. Matviichuk, P. G. Dimitrov, N. G. Bankov, Relativistic Electrons High Doses at International Space Station and Foton M2/M3 Satellites, Adv. Space Res., 44, 1433–1440, 2009. http://dx.doi.org/10.1016/j.asr.2009.09.023
2. Dachev, T. P., Yu. N. Matviichuk, J. V. Semkova, R. T. Koleva, et al., Space radiation dosimetry with active detections for the scientific program of the second Bulgarian cosmonaut on board the Mir space station, Adv. Space Res., 9, 10, 247–251, 1989. http://dx.doi.org/10.1016/0273-1177(89)90445-6
3. Reitz, G. R. Beaujean, E. Benton, S. Burmeister, Ts. Dachev, S. Deme, M. Luszik-Bhadra, and P. Olko, Space radiation measurements on-board ISS—the DOSMAP experiment, Radiat Prot Dosimetry, 116, 374–379, 2005. http://rpd.oxfordjournals.org/cgi/content/abstract/116/1-4/374
4. Dachev, T. P., G. Horneck, D.-P. Häder, M. Lebert, P. Richter, M. Schuster, R. Demets, Time profile of cosmic radiation exposure during the EXPOSE-E mission: the R3D instrument, Journal of Astrobiology, 12, 5, 403–411, 2012. http://dx.doi.org/10.1089/ast.2011.0759
5. Dachev, T. P., G. Horneck, D.-P. Häder, M. Schuster, and M. Lebert, EXPOSE-R cosmic radiation time profile, Journal of Astrobiology, 14, 17–25, 2015. http://dx.doi.org/10.1017/S1473550414000093
6. Dachev, T. P., N. G. Bankov, B. T. Tomov, Y. N. Matviichuk, P. G. Dimitrov, D.-P. Häder, G. Horneck, Overview of the ISS radiation environment observed during the ESA EXPOSE-R2 mission in 2014–2016. Space Weather, 15, 1475–1489, 2017. https://doi.org/10.1002/2016SW001580
7. McIlwain, C.E. (1961). Coordinates for mapping the distribution of magnetically trapped particles. Journal of Geophysical Research, 66, 3681–3691. https://doi.org/10.1029/JZ066i011p03681
8. Heffner, J., 1971. Nuclear Radiation and Safety in Space. M. Atomizdat, p.115 (in Russian).
9. Dachev, T.P., Relativistic electron precipitation bands in the outside radiation environment of the international space station. Journal of Atmospheric and Solar-Terrestrial Physics, 177, pp. 247–256, 2018). https://doi.org/10.1016/j.jastp.2017.11.008
10. Blake, J.B., Looper, M.D., Baker, D.N., Nakamura, R., Klecker, B., Hovestadt, D., 1996. New high temporal and spatial resolution measurements by SAMPEX of the precipitation of relativistic electrons. Adv. Space Res. 18 (8), 171–186.
11. Reitz, G., Beaujean, R., Benton, E., Burmeister, S., Dachev, T., Deme, S., … Olko, P. 2005. Space radiation measurements on-board ISS-the DOSMAP experiment. Radiation Protection Dosimetry, 116, 374–379.
12. Claudepierre, S.G., et al., 2017. The hidden dynamics of relativistic electrons (0.7-1.5 MeV) in the inner zone and slot region. J. Geophys. Res. Space Phys. 122. https://doi.org/10.1002/2016JA023719.
13. Semkova, J., Koleva, R., Benghin, V., Krastev, K., Matviichuk, Y., Tomov, B., Maltchev, S., Dachev, T., Bankov, N., Mitrofanov, I. and Malakhov, A., 2023. Observation of the radiation environment and solar energetic particle events in Mars orbit in May 2018-June 2022. Life Sciences in Space Research. https://doi.org/10.1016/j.lssr.2023.03.006.